Viologen-Modified Platinum Clusters Acting as an Efficient Catalyst in Photocatalytic Hydrogen Evolution

Hiroaki Kotani, Kei Ohkubo, Yoshizo Takai, and Shunichi Fukuzumi*

Department of Material and Life Science, Graduate School of Engineering, Osaka University, SORST, Japan Science and Technology Agency (JST), Suita, Osaka 565-0871, Japan

Received: August 12, 2006; In Final Form: September 20, 2006

A highly efficient photocatalytic system for hydrogen evolution with dihydronicotinamide coenzyme (NADH) as a sacrificial agent in an aqueous solution has been constructed by using water-soluble platinum clusters functionalized with methyl viologen−alkanethiol (MVA^{2+}) and a simple electron-donor dyad, 9-mesityl-10-methylacridinium ion (Acr^{+}−Mes), which is capable of fast photoinduced electron transfer but extremely slow back electron transfer. The mean diameter of the platinum core was determined as $R_{CORE} = 1.9$ nm with a standard deviation $\sigma = 0.5$ nm by transmission electron microscopy (TEM). As a result, the hydrogen-evolution rate of the photocatalytic system with MVA^{2+}-modified platinum clusters (MVA^{2+}−PtC) is 10 times faster than the photocatalytic system with the mixture of the same amount of MVA^{2+} and platinum clusters as that of MVA^{2+}−PtC under otherwise the same experimental conditions. The radical cation of NADH has been successfully detected by laser flash photolysis experiments. The decay of the absorbance due to $NAD^{\bullet}$, produced by the deprotonation from $NADH^{\bullet+}$, coincides with the appearance of the absorption band due to $Acr^{\bullet}$−Mes. This indicates electron transfer from $NAD^{\bullet}$ to Acr^{+}−Mes to give $Acr^{\bullet}$−Mes, which undergoes the electron-transfer reduction of MVA^{2+}−PtC, leading to the efficient hydrogen evolution.

Introduction

Hydrogen (H_2) has merited increased attention as a future energy resource as the global environment issue is becoming one of the important on the agenda of the 21st century, because hydrogen as a fuel is high in energy yet burning hydrogen produces almost zero pollution.[1] A variety of semiconductor metal oxides have so far been studied for water splitting as a means of producing H_2 from water.[2−5] However, these photocatalysts are effective only under ultraviolet (UV) light because of their wide band gap. Since UV light accounts for only a small fraction (5%) of the solar spectrum at the earth's surface, the development of visible-light responsive photocatalysts for water splitting to produce H_2 has attracted much attention.[6−8] Considerable efforts have therefore been made to extend the absorption edge of semiconductors with wide band gaps into the visible region.[9] The quantum efficiency of overall water splitting for hydrogen evolution by photocatalysts has been still too low, and the molecular mechanism has yet to be clarified. On the other hand, molecular photocatalysts have long been explored for the hydrogen evolution using metal complexes as photosensitizers combined with hydrogen-evolution catalysts.[10−17] Although sacrificial donors have so far been required for the molecular photocatalytic hydrogen evolution under visible light irradiation, it is highly desired to improve the photocatalytic efficiency for the hydrogen evolution with electron donors in water. Such molecular photocatalytic hydrogen-production systems consist of an electron donor, a photosensitizer, an electron carrier, and a hydrogen-evolution catalyst. For example, methyl viologen (MV^{2+}) was frequently employed as an electron carrier in combination with a colloidal Pt catalyst for the hydrogen evolution. The important steps in this system are photoinduced electron transfer from a photoexcited photosensitizer to MV^{2+} and the subsequent electron-transfer reduction of colloidal Pt catalyst by the reduced MV^{2+} ($MV^{\bullet+}$). The photoinduced electron-transfer step may be improved by utilizing electron donor−acceptor linked molecules to attain a long-lived charge-separated state, mimicking photoinduced electron-transfer processes in the natural photosynthetic reaction center.[18−22] The efficiency of intermolecular electron transfer from $MV^{\bullet+}$ to colloidal Pt decreases due to the competition with the back electron transfer from $MV^{\bullet+}$ to the oxidized photosensitizer.

We report herein the synthesis and characterization of platinum nanoclusters (MVA^{2+}−PtC), which are directly linked with methyl viologen−alkanethiol (MVA^{2+}), and successful construction of a highly efficient photocatalytic system for hydrogen evolution with dihydronicotinamide coenzyme (NADH) using the water-soluble MVA^{2+}−PtC as a hydrogen evolution catalyst and 9-mesityl-10-methylacridinium ion (Acr^{+}−Mes)[23] as a charge-separation photocatalyst in an aqueous solution. NADH is chosen as an electron source, since NADH plays a key role in a number of biological redox processes including respiratory chain.[24,25] Since ethanol can reduce NAD^{+} to generate NADH in the presence of alcohol dehydrogenases, NADH can be replaced by ethanol as an electron source.[10] The simple electron donor−acceptor dyad (Acr^{+}−Mes) has been reported to undergo efficient photoinduced electron transfer affording an extremely long-lived electron-transfer (ET) state.[23,26,27] The efficient photoinduced electron transfer in Acr^{+}−Mes, combined with much faster intramolecular electron transfer from the $MVA^{\bullet+}$ moiety to the platinum nanoclusters in MVA^{2+}−PtC than intramolecular electron transfer from $MV^{\bullet+}$ to colloidal Pt leads to a highly efficient photocatalytic hydrogen evolution.

* To whom correspondence should be addressed. E-mail: fukuzumi@chem.eng.osaka-u.ac.jp.

10.1021/jp065215v CCC: $33.50
Published on Web 11/09/2006

Experimental Section

Materials. 9-Mesityl-10-methylacridinium perchlorate ($Acr^+-Mes\ ClO_4^-$) was prepared by the reaction of 10-methylacridone in dichloromethane with the Grignard reagents (MesMgBr), followed by addition of sodium hydroxide for the hydrolysis and perchloric acid for the neutralization, and purified by recrystallization from methanol. 4,4′-Bipyridine, methyl iodide, 1,6-dibromohexane, potassium thioacetate, potassium carbonate, 1,4-dihydronicotinamide adenine dinucleotide (NADH), sodium borohydride, and hydrogen hexachloroplatinate(IV) hexahydrate were obtained commercially. Pt−PVP colloid (Pt % = 4.0 wt %) was supplied for Tanaka Kikinzoku Kogyo K.K.[28] Phthalic and phosphate buffer solutions were prepared by 50 mM phthalic acid/NaOH at pH 4.5 and 50 mM KH_2PO_3/NaOH at pH 7.0 and 6.0, respectively.

1-Methyl-4,4′-bipyridinium Iodide (1). 1-Methyl-4,4′-bipyridinium iodide was synthesized by stirring 4,4′-bipyridine (10 g, 64 mmol) and methyl iodide (9.0 g, 64 mmol) in acetone (300 mL). After the filtration, the residue was washed with acetonitrile to afford 15 g (yield: 79%) of a yellow solid. ^{1}H NMR (300 MHz, CD_3CN) δ 8.83 (d, 2H, J = 6.0 Hz), 8.75 (d, 2H, J = 6.0 Hz), 8.30 (d, 2H, J = 6.0 Hz), 7.78 (d, 2H, J = 6.0 Hz), 4.34 (s, 3H). Anal. Calcd for $C_{11}H_{11}IN_2$: C, 44.32; H, 3.72; N, 9.40. Found: C, 44.22; H, 3.59; N, 9.36. MALDI-TOF-MS: m/z [M − I$^-$] calcd for $C_{11}H_{11}N_2$, 171.1; found, 171.5.

Thioacetic Acid *S*-(6-Bromohexyl) Ester (2). A solution of potassium thioacetate (2 g, 0.18 mmol) in ethanol (100 mL) was added to 1,6-dibromohexane (8 g, 35 mmol). The reaction mixture was stirred overnight at room temperature. The solvent was evaporated under reduced pressure after filtration, giving a colorless oil. The oil was purified by column chromatography (20:1 (v/v) hexanes/$CHCl_3$) to give 3.4 g of **2** as a colorless oil (yield: 40%). ^{1}H NMR (300 MHz, $CDCl_3$) δ 3.40 (t, 2H, J = 6.0 Hz), 2.86 (t, 2H, J = 6.0 Hz), 2.32 (s, 3H), 1.85 (m, 2H), 1.59 (m, 2H), 1.42 (m, 4H).

1-(1-Hexyl-6-thioacetate)-1′-methyl-4,4′-bipyridinium (3). A mixture of **1** (0.9 g, 3 mmol) and **2** (0.72 g, 3 mmol) in DMF (50 mL) was stirred for 12 h at 353 K. The solvent was evaporated under reduced pressure and washed with acetonitrile to afford 0.5 g (yield: 32%) of a red solid. ^{1}H NMR (300 MHz, D_2O) δ 8.96 (d, 2H, J = 6.0 Hz), 8.90 (d, 2H, J = 6.0 Hz), 8.39 (m, 4H), 4.36 (s, 3H), 2.72 (t, 2H, J = 6.0 Hz), 2.20 (s, 3H), 1.95 (m, 2H), 1.44 (m, 2H), 1.27 (m, 4H). Anal. Calcd for $C_{19}H_{26}BrIN_2OS\cdot 0.25(H_2O)$: C, 42.12; H, 4.93; N, 5.17. Found: C, 41.50; H, 4.57; N, 5.16. MALDI-TOF-MS: m/z [M − Br$^-$, I$^-$] calcd for $C_{19}H_{26}N_2OS$, 330.2; found, 330.3.

1-(1-Hexyl-6-thiol)-1′-methyl-4,4′-bipyridinium Dinitrates (MVA^{2+}). An aqueous solution (10 mL) of **3** (0.1 g, 0.2 mmol) was added to an aqueous solution of K_2CO_3 (0.1 g, 1.0 mmol). The solution was stirred vigorously for 2 h, and some drops of HNO_3 were added to the solution for the neutralization to give MVA^{2+} (yield: 61%) of a brown solid. ^{1}H NMR (300 MHz, D_2O) δ 8.96 (d, 2H, J = 6.0 Hz), 8.90 (d, 2H, J = 6.0 Hz), 8.39 (m, 4H), 4.36 (s, 3H), 2.70 (t, 1H, J = 6.0 Hz), 2.56 (t, 2H, J = 6.0 Hz), 1.94 (m, 2H), 1.52 (m, 2H), 1.27 (m, 4H). MALDI-TOF-MS: m/z [M − 2NO$_3^-$] calcd for $C_{17}H_{24}N_2S$, 288.2; found, 288.6.

MVA^{2+}-Modified Platinum Clusters ($MVA^{2+}-PtC$). $MVA^{2+}-PtC$ was prepared as shown in Scheme 2. Using a 1:1 MVA^{2+}/Pt mole ratio, 0.041 g (0.1 mmol) of MVA^{2+} and 0.040 g (0.1 mmol) of $H_2PtCl_4\cdot 6H_2O$ were stirred into 5 mL of water. The solution was allowed to stir for 30 min before a solution of $NaBH_4$ (0.1 g, 2.7 mmol) dissolved in 2 mL of water was added. An immediate appearance of dark brown color indicated the formation of clusters. After stirring for an additional 30 min, the mixture was evaporated under a vacuum to near dryness, and then the particles were purified by sephadex (G10) column chromatography (3.0 × 20 cm) and eluted with distilled water. Anal. Found: C, 19.91; H, 2.69; N, 3.25.

SCHEME 1

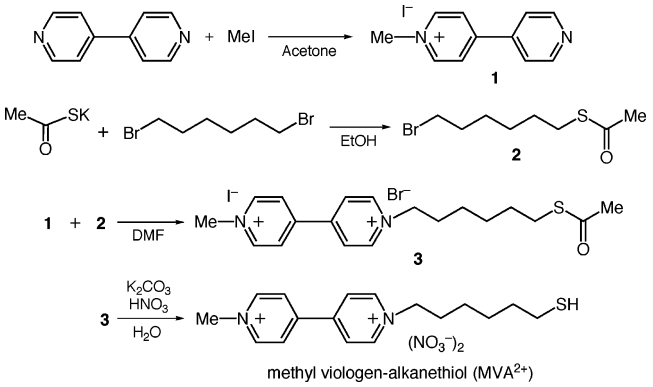

SCHEME 2

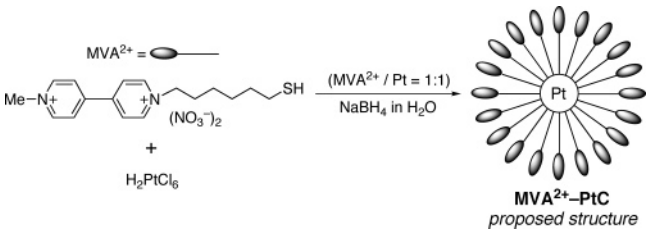

Transmission Electron Microscopy (TEM). The diameters of platinum clusters were determined from bright field images using an HF-2000 (HITACHI) that has a cold field emission gun with an accelerating voltage of 200 kV. The sample was prepared by dropping an aqueous solution of $MVA^{2+}-PtC$ and allowing the solvent to evaporate and then scooped up with the amorphous carbon supporting film.

Electrochemical Measurements. Electrochemical measurements were performed on an ALS630B electrochemical analyzer in deaerated water containing 0.01 M Na_2SO_4 as supporting electrolyte at 298 K. A conventional three-electrode cell was used with a platinum working electrode (BAS, surface area of 0.3 mm^2) and a platinum wire as the counter electrode. The Pt working electrode was routinely polished with alumina suspension and rinsed with acetone before use. The measured potentials were recorded with respect to the Hg/Hg_2Cl_2 (saturated KCl solution) reference electrode (vs SCE).

Spectral Measurements. UV−visible absorption spectra of an aqueous solution of $MVA^{2+}-PtC$ and MVA^{2+} were recorded using a Hewlett-Packard 8453 diode array spectrophotometer with a quartz cuvette (path length = 10 mm) at 298 K. A capped quartz cuvette was used for all experiments. Absorption spectra of the viologen radical cation were measured after 5 min of deoxygenation in flowing Ar, followed by the addition of $Na_2S_2O_4$ (1.0×10^{-2} M) in water. Rates of intramolecular electron-transfer reactions from $MVA^{\bullet+}$ to platinum clusters in buffer solution of $MVA^{2+}-PtC$ were determined by monitoring a decrease in absorbance at 600 nm due to $MVA^{\bullet+}$.

Time-Resolved Absorption Measurements. A deaerated MeCN/buffer solution at pH 4.5 (1:1 v/v) containing NADH (1.0×10^{-4} M) and Acr^+-Mes (2.0×10^{-5} M) was excited by a Nd:YAG laser (Continuum, SLII-10, 4−6 ns fwhm) at λ = 355 nm with the power of 5 mJ per pulse. The transient absorption measurements were performed using a continuous

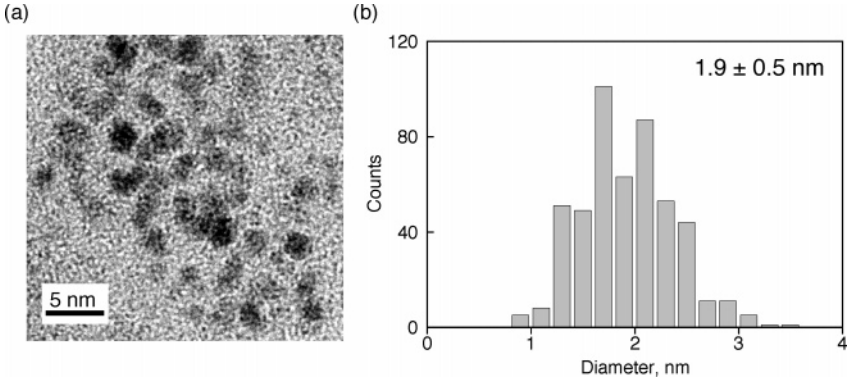

Figure 1. (a) Transmission electron microscopy (TEM) image and (b) core size histograms of MVA^{2+}−PtC.

xenon lamp (150 W) and a photomultiplier (Hamamatsu 2949) as a probe light and a detector, respectively. The output from a photomultiplier was recorded on a digitizing oscilloscope (Tektronix, TDS3032, 300 MHz).

Photocatalytic Hydrogen Evolution. The phthalic acid buffer (pH 4.5) solution (2 mL) containing MVA^{2+}−PtC (0.5 mg dm^{-3}), NADH (2.0×10^{-3} M), and Acr^+−Mes (2.0×10^{-4} M) was deaerated by freeze−pump−thaw cycles (three times) and flushed with argon gas. The solution was then irradiated with a xenon lamp (Ushio Optical ModelX SX-UID 500XAMQ) through a color filter glass (Asahi Techno Glass L39) transmitting $\lambda > 390$ nm at room temperature. The amounts of hydrogen were determined using a Shimadzu GC-14B gas chromatography (detector, TCD; column temperature, 50 °C; column, active carbon with the particle size 60−80 mesh; carrier gas, nitrogen gas). As a reference system, H_2 evolution was also examined using the same amount of mixture of MVA^{2+} (2.5×10^{-4} M) and Pt−PVP colloid (7.5 mg dm^{-3}), instead of MVA^{2+}−PtC (0.5 mg dm^{-3}) in a phthalic acid buffer (pH 4.5) solution (2 mL) containing NADH (2.0×10^{-3} M) and Acr^+−Mes (2.0×10^{-4} M). The Pt concentration of MVA^{2+}−PtC (0.5 mg dm^{-3}) is 0.30 mg dm^{-3}, which is taken as the same as that of Pt−PVP colloid (0.30 mg dm^{-3}). The MVA^{2+} concentration of MVA^{2+}−PtC (2.5×10^{-4} M) was determined by the ratio of MVA^{2+}/MVA^{2+}−PtC wt % of 0.403.

Results and Discussion

Methyl Viologen-Modified Platinum Clusters. The synthetic route to methyl viologen−alkanethiol (MVA^{2+}) is summarized in Scheme 1 (see Experimental Section). The methyl viologen-modified platinum clusters (MVA^{2+}−PtC) were prepared by applying the same method as the preparation of alkanethiolate-modified gold nanoparticles,[29,30] that is, the reduction of H_2PtCl_4 with $NaBH_4$ in water containing MVA^{2+} ($MVA^{2+}/H_2PtCl_4 = 1{:}1$), as shown in Scheme 2. MVA^{2+}−PtC was purified by sephadex (G10) column chromatography and characterized by ^{1}H NMR and elemental analysis (see Experimental Section).

The mean diameter of the platinum core ($2R_{CORE}$) was determined by transmission electron microscopy (TEM) as shown in Figure 1. The average diameter of the MVA^{2+}−PtC is in the 1.9 nm range, which is similar to the diameter reported for the water-soluble platinum clusters.[31] MVA^{2+}−PtC with the diameter of 1.9 nm is comprised of 210 platinum atoms, of which 130 lie on the Pt surface.[32] The number of MVA^{2+} on the Pt surface is determined as 67 from the elemental analysis of MVA^{2+}−PtC (see Experimental Section).

The ^{1}H NMR spectrum of MVA^{2+}−PtC was measured in D_2O as shown in Figure 2, together with that of MVA^{2+} in

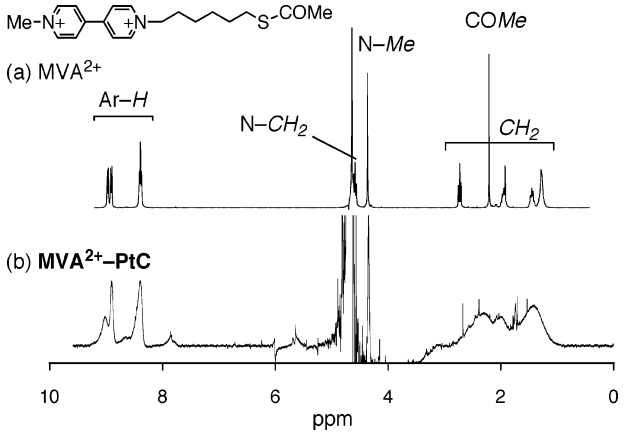

Figure 2. ^{1}H NMR spectra of (a) MVA^{2+} and (b) MVA^{2+}−PtC in D_2O.

D_2O for comparison. The complete disappearance of the −COMe signal of **3** at 2.20 ppm in MVA^{2+}−PtC due to significant broadening of the sharp signal observed in MVA^{2+} indicates that virtually all the MVA^{2+} molecules are covalently linked to the platinum surface to leave no free MVA^{2+} molecules.

One-Electron Reduction Potentials of MVA^{2+}−PtC and MVA^{2+}. The cyclic voltammograms of MVA^{2+}−PtC and MVA^{2+} (2.0×10^{-3} M) were measured in deaerated water containing 0.01 M Na_2SO_4, and the data are shown in Supporting Information, Figure S1. The first one-electron reduction potential of MVA^{2+}−PtC was observed at −0.50 V vs SCE which is significantly shifted to a positive direction as compared with that of MVA^{2+} (−0.67 V). Such a positive shift in the E^0_{red} value of MVA^{2+}−PtC indicates that MVA^{2+} molecules in MVA^{2+}−PtC are less solvated due to the close packing of MVA^{2+} molecules on the Pt surface as compared with free MVA^{2+} molecules in solution.

The UV−vis spectra of MVA^{2+}−PtC and MVA^{2+} are shown in Figure 3 together with those of $MVA^{\bullet+}$−PtC and $MVA^{\bullet+}$, which are produced by the reduction of MVA^{2+}−PtC and MVA^{2+} by $Na_2S_2O_4$ in aqueous solution at pH 7.0, respectively. The absorption band of $MVA^{\bullet+}$−PtC (525 nm) is blue-shifted from 605 nm due to $MVA^{\bullet+}$ to 525 nm. Such a blue shift may result from the $\pi-\pi$ interaction between closely packed $MVA^{\bullet+}$ molecules on the Pt surface.[33]

Once $MVA^{\bullet+}$−PtC is generated, the hydrogen (H_2) evolution may occur by intramolecular electron transfer from the methyl viologen radical cation to platinum and the two-electron reduction of two protons on the platinum surface (Scheme 3). The decay of the absorption spectrum at 525 nm due to $MVA^{\bullet+}$−PtC obeys zero-order kinetics, which is dependent on

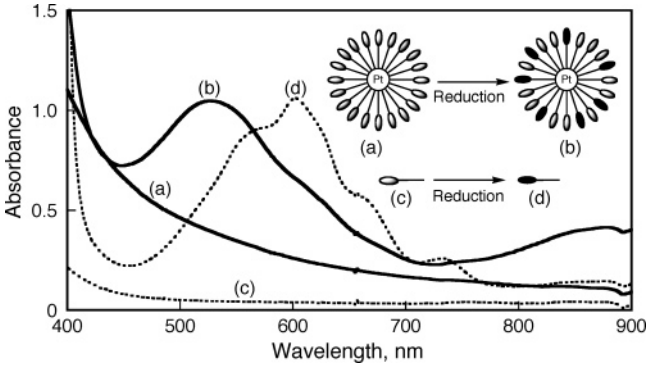

Figure 3. UV−vis spectra of (a) MVA^{2+}−PtC, (b) $MVA^{\bullet+}$−PtC, (c) MVA^{2+}, and (d) $MVA^{\bullet+}$ in aqueous solution at pH 7.0.

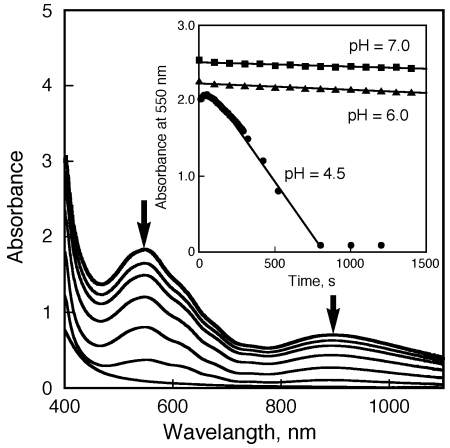

Figure 4. Vis−NIR spectral changes of $MVA^{\bullet+}$−PtC in water at pH 4.5 followed by addition of $Na_2S_2O_4$. Inset: pH dependence of the decay time profile at 550 nm.

SCHEME 3

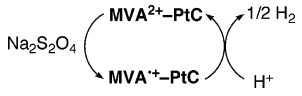

the pH in buffer solutions as shown in Figure 4. The rate of H_2 evolution at pH 4.5 is about 40 times larger than that at pH 7.0. This indicates that the rate-determining step is not electron transfer from viologen radical cation to the platinum but electron transfer from the platinum to the proton.

Photocatalytic Hydrogen Evolution. The hydrogen-evolution efficiency was tested using the photocatalytic system composed of NADH and MVA^{2+}−PtC at pH 4.5 (Figure 5, ●), since the efficient hydrogen evolution was observed for the reduced MVA^{2+}−PtC at pH 4.5 (vide supra). As a reference system, the hydrogen-evolution efficiency was also determined using a mixture of the same amounts of MVA^{2+} and Pt−PVP colloid under the same experimental conditions as employed for the NADH/MVA^{2+}−PtC system (Figure 5, ■). The concentration of MVA^{2+} was adjusted as 2.5×10^{-4} M which is the same as the concentration of MVA^{2+} contained in MVA^{2+}−PtC (0.5 mg dm^{-3}); see Experimental Section. The amount of Pt−PVP colloid was also adjusted as 7.5 mg dm^{-3}, in which the amount of Pt metal is the same as that contained in MVA^{2+}−PtC (0.5 mg dm^{-3}). The amount of H_2 evolution of the NADH/MVA^{2+}−PtC system increases with photoirradiation time linearly as shown in Figure 5, and the rate was estimated to be 2.4 μmol h^{-1}, which is 10 times faster than the rate of the NADH/MVA^{2+}/Pt−PVP colloid system.

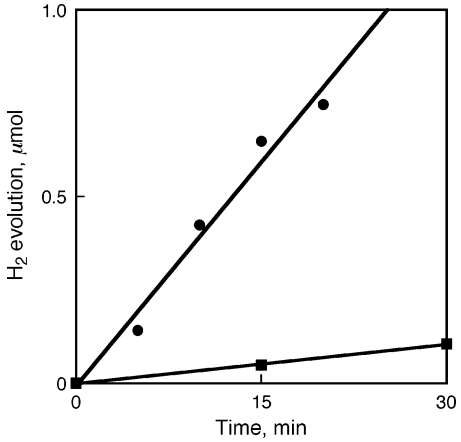

Figure 5. Time dependence of hydrogen evolution under photoirradiation ($\lambda > 390$ nm) to the aqueous buffer solution at pH 4.5 containing Acr^{+}−Mes (2.0×10^{-4} M) and NADH (2.0×10^{-3} M) with MVA^{2+}−PtC (●) and with the same amounts of Pt−PVP colloid and MVA^{2+} (■).

SCHEME 4

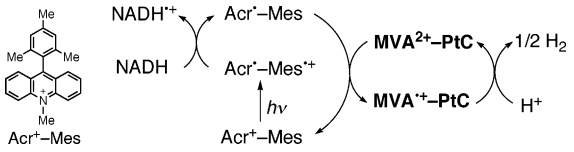

Scheme 4 shows the mechanism of hydrogen evolution in the NADH/MVA^{2+}−PtC system. First the photoirradiation of Acr^{+}−Mes results in formation of the electron-transfer state ($Acr^{\bullet}$−$Mes^{\bullet+}$). This undergoes the electron-transfer oxidation of NADH and/or the electron-transfer reduction of MVA^{2+} in MVA^{2+}−PtC. Both processes are thermodynamically feasible, because the one-electron oxidation potential of NADH (E^0_{ox} = 0.76 V vs SCE)[34,35] is less positive than the one-electron reduction potential of the $Mes^{\bullet+}$ moiety of $Acr^{\bullet}$−$Mes^{\bullet+}$, and the one-electron oxidation potential of the $Acr^{\bullet}$ moiety (E^0_{ox} = −0.57 V vs SCE)[36] is more negative than the one-electron reduction potential of the MVA^{2+} moiety in MVA^{2+}−PtC (E^0_{red} = −0.50 V). In contrast, however, electron transfer from $Acr^{\bullet}$−$Mes^{\bullet+}$ (E^0_{ox} = −0.57 V vs SCE) to MV^{2+} (E^0_{red} = −0.67 V) is energetically unfavorable, because the E^0_{ox} value of $Acr^{\bullet}$−$Mes^{\bullet+}$ is more positive than the E^0_{red} value of MV^{2+}. In this case, MV^{2+} may be reduced by $NAD^{\bullet}$, which is produced via deprotonation of $NADH^{\bullet+}$, since the electron transfer from $NAD^{\bullet}$ (E^0_{ox} = −1.1 V vs SCE)[34,35] to MV^{2+} (E^0_{red} = −0.67 V) is highly exergonic. Thus, $Acr^{\bullet}$−$Mes^{\bullet+}$ is more efficiently quenched in the NADH/MVA^{2+}−PtC system as compared with the NADH/MV^{2+}/Pt−PVP colloid system. In addition, the electron injection from $MVA^{\bullet+}$ to Pt clusters is certainly more efficient in the MVA^{2+}−bound Pt clusters as compared with intermolecular electron transfer from $MV^{\bullet+}$ to Pt−PVP colloid in solution, leading to the 10 times faster H_2 evolution (Figure 5).

Detection of Photocatalytic Intermediates. To confirm the electron-transfer processes in Scheme 4, the intermediate radicals and radical cations are detected by laser flash photolysis experiments. Nanosecond laser excitation at 355 nm of a deaerated aqueous solution of Acr^{+}−Mes results in formation of the electron-transfer state ($Acr^{\bullet}$−$Mes^{\bullet+}$) via photoinduced electron transfer from the Mes moiety to the singlet excited state of the Acr^{+} moiety.[23] The quantum yields for the formation of $Acr^{\bullet}$−$Mes^{\bullet+}$ has previously been determined as almost quantitative (98%) in MeCN.[23] The transient absorption spectra obtained

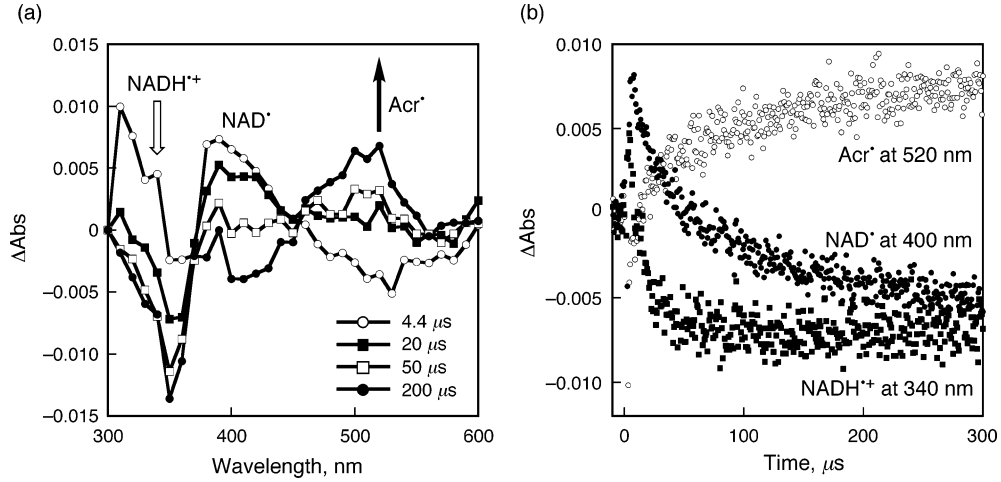

Figure 6. (a) Transient absorption spectra of Acr^+-Mes (2.0×10^{-5} M) in deaerated MeCN/buffer solution at pH 4.5 (1:1 v/v) in the presence of NADH (1.0×10^{-4} M) at 298 K taken at 4.4 (○), 20 (■), 50 (□), and 200 μs (●) after laser excitation at 355 nm. (b) Absorbance time profiles at 350 nm due to $NADH^{\bullet+}$ (■), at 400 nm due to $NAD^{\bullet}$ (●), and at 520 nm due to $Acr^{\bullet}$ (○).

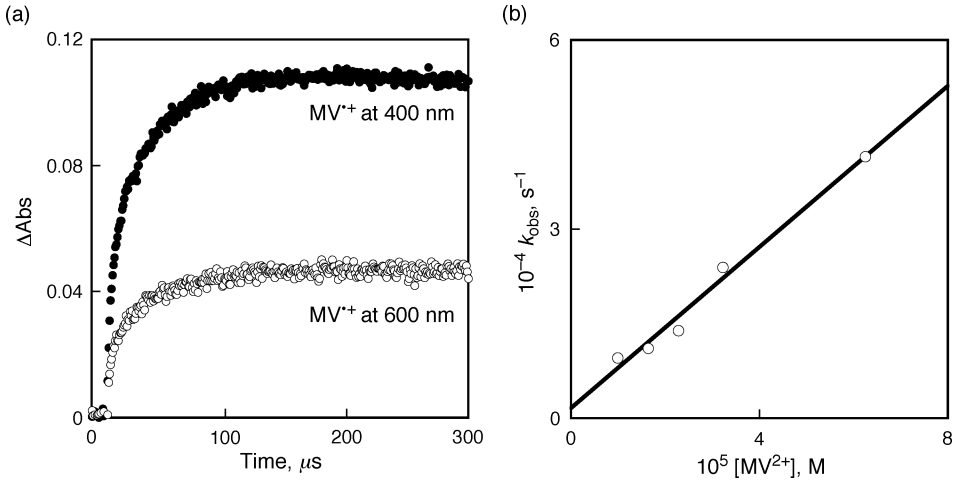

Figure 7. (a) Absorbance time profiles at 400 and 600 nm due to $MV^{\bullet+}$ in deaerated MeCN/buffer solution at pH 4.5 (1:1 v/v) in the presence of NADH (1.0×10^{-4} M), MV^{2+} (6.0×10^{-5} M), and Acr^+-Mes (2.0×10^{-5} M) at 298 K after laser excitation at 355 nm. (b) Plot of the pseudo-first-order rate constant (k_{obs}) for electron transfer from the $Acr^{\bullet}$ moiety of $Acr^{\bullet}-Mes^{\bullet+}$ to MV^{2+} vs $[MV^{2+}]$.

SCHEME 5

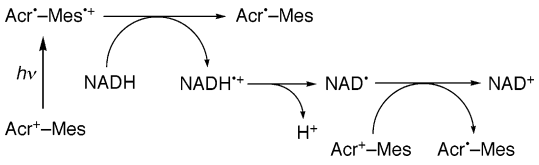

after laser excitation of a deaerated MeCN/buffer solution at pH 4.5 (1:1 v/v) containing Acr^+-Mes (2.0×10^{-5} M) and NADH (1.0×10^{-4} M) exhibits the appearance of a new transient absorption band at 340 nm as shown in Figure 6a. The newly formed absorption band at 340 nm in the presence of NADH is assigned to that of $NADH^{\bullet+}$, since a similar absorption band has been reported for the radical cation of an NADH model compound.[37] Thus, electron transfer from NADH to $Acr^{\bullet}-Mes^{\bullet+}$ occurs to produce $NADH^{\bullet+}$ (Scheme 5). On the other hand, the absorption band due to the $Acr^{\bullet}$ moiety at 520 nm[23] remains virtually the same in the absence of NADH. The coincidence of the fast decay of the absorbance at 340 nm due to $NADH^{\bullet+}$ and the appearance of the absorption band at 400 nm due to $NAD^{\bullet}$ indicates that $NADH^{\bullet+}$ deprotonates to produce $NAD^{\bullet}$ (Scheme 5).[35] Then, electron transfer from $NAD^{\bullet}$ ($E^0_{ox} = -1.1$ V vs SCE)[34] to the Acr^+ moiety in Acr^+-Mes ($E^0_{red} = -0.57$ V vs SCE) results in the formation of the $Acr^{\bullet}$ moiety in $Acr^{\bullet}-Mes$ ($Acr^{\bullet}$: $\lambda_{max} = 520$ nm) with a concomitant decrease in the absorption band due to the $NAD^{\bullet}$ ($NAD^{\bullet}$: $\lambda_{max} = 400$ nm)[38] as shown in Figure 6.

When MV^{2+} (6.0×10^{-5} M) is added to the NADH/Acr^+-Mes system, efficient electron transfer from $NAD^{\bullet}$ to MV^{2+} is observed as indicated by the rise in absorbance at 400 and 600 nm due to $MV^{\bullet+}$ as shown in Figure 7a. The disappearance of absorbance at 400 nm due to $NAD^{\bullet}$ is overlapped with that of the absorbance due to $MV^{\bullet+}$, which has a higher extinction coefficient ($\epsilon = 4.5 \times 10^4$ M^{-1} cm^{-1}).[33] The second-order rate constant of electron transfer from $NAD^{\bullet}$ to MV^{2+} is determined as 6.4×10^8 M^{-1} s^{-1} from the slope of a linear plot of the pseudo-first-order rate constant versus concentration of MV^{2+} (Figure 7b).

In contrast to the efficient electron transfer from NADH to $Acr^{\bullet}-Mes^{\bullet+}$ (Figure 6), electron transfer from the $Acr^{\bullet}$ moiety of $Acr^{\bullet}-Mes^{\bullet+}$ to MV^{2+} hardly occurs as indicated by the comparison of the time profile of absorbance at 400 nm obtained after laser excitation of a deaerated aqueous solution of Acr^+-Mes (2.0×10^{-5} M) containing NADH (1.0×10^{-4} M) with that containing MV^{2+} (6.0×10^{-5} M); see Supporting Information, Figure S2. This is consistent with the fact that the electron transfer from the $Acr^{\bullet}$ moiety of $Acr^{\bullet}-Mes^{\bullet+}$ to MV^{2+} is thermodynamically unfavorable (vide supra).

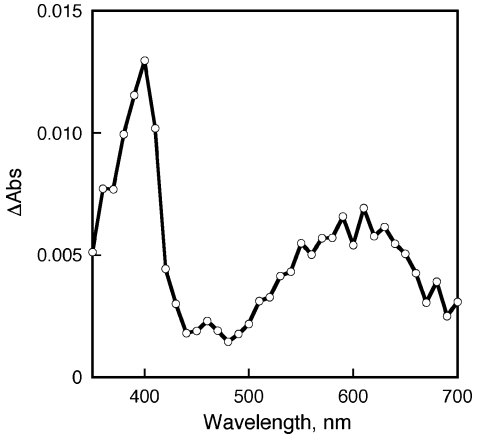

Figure 8. Transient absorption spectrum of Acr^+-Mes (2.0×10^{-5} M) in deaerated aqueous buffer solution at pH 4.5 in the presence of $MVA^{2+}-PtC$ (0.5 mg dm^{-3}) taken at 35 μs after laser excitation at 355 nm.

When $MVA^{2+}-PtC$ is added to an aqueous solution of Acr^+-Mes instead of MV^{2+}, however, efficient electron transfer from the $Acr^•$ moiety of $Acr^•-Mes^{•+}$ to $MVA^{2+}-PtC$ occurs as indicated by the rise in absorbance at 400 and 600 nm due to $MVA^{•+}-PtC$ (Figure 8).

Conclusions

In conclusion, we have demonstrated the highly efficient H_2 evolution system by using $MVA^{2+}-PtC$, combined with Acr^+-Mes, which is capable of fast charge separation and extremely slow charge recombination.[23] The efficient electron-transfer oxidation of NADH and the reduction of $MVA^{2+}-PtC$ by the electron-transfer state ($Acr^•-Mes^{•+}$), together with the direct electron injection from the $MVA^{•+}$ moiety to the Pt clusters in the $MVA^{2+}-$bound Pt clusters, leads to 10 times more efficient hydrogen evolution as compared with the photocatalytic system composed of separate mixtures of the same amounts of MV^{2+} and Pt clusters. Although the use of water as an electron source has yet to be achieved, NADH is readily replaced by other electron donors such as ethanol by combination with alcohol dehydrogenase which catalyzes the reduction of NAD^+ to NADH with an excess amount of alcohol;[39] the present photocatalytic system composed of NADH, Acr^+-Mes, and $MVA^{2+}-PtC$ makes it among the most promising photocatalytic systems available for H_2 evolution under visible light irradiation.

Acknowledgment. This work was partially supported by a Grant-in-Aid (Nos. 17750039) from the Ministry of Education, Culture, Sports, Science and Technology, Japan.

Supporting Information Available: The cyclic voltammograms of MVA^{2+} and $MVA^{2+}-PtC$ and time profile of absorbance at 400 nm due to $MV^{•+}$. This material is available free of charge via the Internet at http://pubs.acs.org.

References and Notes

(1) Fujishima, A.; Honda, K. *Nature (London)* **1972**, *238*, 37.

(2) Takata, T.; Furumi, Y.; Shinohara, K.; Tanaka, A.; Hara, M.; Kondo, J. N.; Domen, K. *Chem. Mater.* **1997**, *9*, 1063.

(3) (a) Kato, K.; Asakura, K.; Kudo, A. *J. Am. Chem. Soc.* **2003**, *125*, 3082. (b) Ishikawa, A.; Takata, T.; Kondo, J. N.; Hara, M.; Kobayashi, H.; Domen, K. *J. Am. Chem. Soc.* **2002**, *124*, 13547.

(4) Zou, Z.; Ye, J.; Sayama, K.; Arakawa, H. *Nature (London)* **2001**, *414*, 625.

(5) (a) Lei, Z.; You, W.; Liu, M.; Zhou, G.; Takata, T.; Hara, M.; Domen, K.; Li, C. *Chem. Commun.* **2003**, 2142. (b) Liu, M.; You, W.; Lei, Z.; Zhou, G.; Yang, J.; Wu, G.; Ma, G.; Luan, G.; Takata, T.; Hara, M.; Domen, K.; Li, C. *Chem. Commun.* **2004**, 2192.

(6) (a) Hwang, D. W.; Kim, H. G.; Lee, J. S.; Kim, J.; Li, W.; Oh, S. H. *J. Phys. Chem. B* **2005**, *109*, 2093. (b) Shangguan, W.; Yoshida, A. *J. Phys. Chem. B* **2002**, *106*, 12227. (c) Tsuji, I.; Kato, H.; Kudo, A. *Chem. Mater.* **2006**, *18*, 1969.

(7) (a) Anpo, M. *Catal. Surv. Jpn.* **1997**, *1*, 169. (b) Kudo, A. *Int. J. Hydrogen Energy* **2006**, *31*, 197.

(8) (a) Lu, D.; Takata, T.; Saito, N.; Inoue, Y.; Domen, K. *Nature (London)* **2006**, *440*, 295. (b) Asahi, R.; Morikawa, T.; Ohwaki, T.; Aoki, K.; Taga, Y. *Science* **2001**, *293*, 269.

(9) Grätzel, M.; Moser, J.-E. In *Electron Transfer in Chemistry*; Balzani, V., Ed.; Wiley-VCH: Weinheim, Germany, 2001; Vol. 5, pp 589−644.

(10) Handman, J.; Harriman, A.; Porter, G. *Nature (London)* **1984**, *307*, 534.

(11) Darwent, J. R.; Douglas, P.; Harriman, A.; Porter, G.; Richoux, M.-C. *Coord. Chem. Rev.* **1982**, *44*, 83.

(12) Kiwi, J.; Kalyanasundram, K.; Grätzel, M. *Struct. Bonding (Berlin)* **1982**, *49*, 37.

(13) Okura, I. *Coord. Chem. Rev.* **1985**, *68*, 53.

(14) Okura, I. *Photosensitization of Porphyrins and Phthalocyanines*; Kodansha: Tokyo, 2000.

(15) Amao, Y.; Okura, I. *J. Mol. Catal. B: Enzym.* **2002**, *17*, 9.

(16) Okura, I.; Hosono, H. *J. Phys. Chem.* **1992**, *96*, 4466.

(17) (a) Jiang, D.-L.; Choi, C.-K.; Honda, K.; Li, W.-S.; Yuzawa, T.; Aida, T. *J. Am. Chem. Soc.* **2004**, *126*, 12084. (b) Himeshima, N.; Amao, Y. *Energy Fuels* **2003**, *17*, 1641. (c) Astuti, Y.; Palomares, E.; Haque, S. A.; Durrant, J. R. *J. Am. Chem. Soc.* **2005**, *127*, 15120.

(18) Wasielewski, M. R. *Chem. Rev.* **1992**, *92*, 435.

(19) (a) Gust, D.; Moore, T. A.; Moore, A. L. In *Electron Transfer in Chemistry*; Balzani, V., Ed.; Wiley-VCH: Weinheim, 2001; Vol. 3, pp 272−336. (b) Gust, D.; Moore, T. A. In *The Porphyrin Handbook*; Kadish, K. M., Smith, K. M., Guilard, R., Eds.; Academic Press: San Diego, CA, 2000; Vol. 8, pp 153−190. (c) Gust, D.; Moore, T. A.; Moore, A. L. *Acc. Chem. Res.* **2001**, *34*, 40.

(20) (a) Jordan, K. D.; Paddon-Row, M. N. *Chem. Rev.* **1992**, *92*, 395. (b) Paddon-Row, M. N. *Acc. Chem. Res.* **1994**, *27*, 18. (c) Paddon-Row, M. N. *Adv. Phys. Org. Chem.* **2003**, *38*, 1. (d) Verhoeven, J. W. *Adv. Chem. Phys.* **1999**, *106*, 603.

(21) (a) Harriman, A.; Sauvage, J.-P. *Chem. Soc. Rev.* **1996**, *25*, 41. (b) Blanco, M.-J.; Consuelo Jiménez, M.; Chambron, J.-C.; Heitz, V.; Linke, M.; Sauvage, J.-P. *Chem. Soc. Rev.* **1999**, *28*, 293.

(22) (a) Fukuzumi, S.; Guldi, D. M. In *Electron Transfer in Chemistry*; Balzani, V., Ed.; Wiley-VCH: Weinheim, 2001; Vol. 2, pp 270−337. (b) Fukuzumi, S. *Org. Biomol. Chem.* **2003**, *1*, 609. (c) Fukuzumi, S. *Bull. Chem. Soc. Jpn.* **2006**, *79*, 177.

(23) Fukuzumi, S.; Kotani, H.; Ohkubo, K.; Ogo, S.; Tkachenko, N. V.; Lemmetyinen, H. *J. Am. Chem. Soc.* **2004**, *126*, 1600.

(24) (a) Kotani, H.; Ohkubo, K.; Fukuzumi, S. *J. Am. Chem. Soc.* **2004**, *126*, 15999. (b) Ohkubo, K.; Nanjo, T.; Fukuzumi, S. *Org. Lett.* **2005**, *7*, 4265.

(25) The ET state of Acr^+-Mes has been suggested to be the local excited (LE) triplet state; see (a) Benniston, A. C.; Harriman, A.; Li, P.; Rostron, J. P.; Verhoeven, J. W. *Chem. Commun.* **2005**, 2701. (b) Benniston, A. C.; Harriman, A.; Li, P.; Rostron, J. P.; van Ramesdonk, H. J.; Groeneveld, M. M.; Zhang, H.; Verhoeven, J. W. *J. Am. Chem. Soc.* **2005**, *127*, 16054. However, the reported triplet excited state has been shown to result from the acridine impurity contained in Acr^+-Mes; see: (c) Ohkubo, K.; Kotani, H.; Fukuzumi, S. *Chem. Commun.* **2005**, 4520.

(26) (a) Saraste, M. *Science* **1999**, *283*, 1488. (b) Walker, J. E. *Q. Rev. Biophys.* **1992**, *25*, 253. (c) Hirst, J. *Proc. Natl. Acad. Sci. U.S.A.* **2003**, *100*, 773.

(27) Fukuzumi, S. *Advances in Electron-Transfer Chemistry*; JAI Press, Inc.: Greenwich, CT, 1992; Vol. 2, pp 67−175.

(28) Toshima, N.; Hirakawa, K. *Polym. J.* **1999**, *31*, 1127.

(29) (a) Templeton, A. C.; Cliffel, D. E.; Murray, R. W. *J. Am. Chem. Soc.* **1999**, *121*, 7081. (b) Cliffel, D. E.; Zamborini, F. P.; Gross, S. M.; Murray, R. W. *Langmuir* **2000**, *16*, 9699. (c) Templeton, A. C.; Chen, S.; Gross, S. M.; Murray, R. W. *Langmuir* **1999**, *15*, 66.

(30) Imahori, H.; Kashiwagi, Y.; Hanada, T.; Endo, Y.; Nishimura, Y.; Yamazaki, I.; Fukuzumi, S. *J. Mater. Chem.* **2003**, *13*, 2890.

(31) (a) Eklund, S. E.; Cliffel, D. E. *Langmuir* **2004**, *20*, 6012. (b) Chen, S.; Kimura, K. *J. Phys. Chem. B* **2001**, *105*, 5397. (c) Li, Y.; Petroski, J.; El-Sayed, M. A. *J. Phys. Chem. B* **2000**, *104*, 10956.

(32) The number of platinum atoms in $MVA^{2+}-PtC$ is determined by the equation ($= \rho_{Pt}4/3(\pi R_{CORE}^3)$) with density ρ_{Pt} (58.01 atoms/nm^3), see: Terrill, R. H.; Postlethwaite, T. A.; Chen, C.-h.; Poon, C.-D.; Terzis, A.; Chen, A.; Hutchison, J. E.; Clark, M. R.; Wignall, G.; Londono, J. D.; Superfine, R.; Falvo, M.; Johnson, C. S., Jr.; Samulski, E. T.; Murray, R. W. *J. Am. Chem. Soc.* **1995**, *117*, 12537.

(33) Baker, W. S.; Lemon, B. I., III; Crooks, R. M. *J. Phys. Chem. B* **2001**, *105*, 8885.

(34) Zhu, X.-Q.; Yang, Y.; Zhang, M.; Cheng, J.-P. *J. Am. Chem. Soc.* **2003**, *125*, 15298.

(35) Fukuzumi, S.; Tanaka, T. *Photoinduced Electron Transfer*; Fox, M. A., Chanon, M., Eds.; Elsevier: Amsterdam, 1988; Part C, Chapter 10.

(36) The one-electron reduction potential of Acr^+-Mes was determined by the cyclic voltammetry measurements as −0.50 V vs SCE in water containing 10 mM Na_2SO_4 and −0.57 V vs SCE in MeCN containing 0.1 M TBAP.

(37) (a) Fukuzumi, S.; Inada, O.; Suenobu, T. *J. Am. Chem. Soc.* **2002**, *124*, 14538. (b) Fukuzumi, S.; Inada, O.; Suenobu, T. *J. Am. Chem. Soc.* **2003**, *125*, 4808.

(38) For similar absorption bands due to $NAD^•$ analogues, see: (a) Hermolin, J.; Levin, M.; Kosower, E. M. *J. Am. Chem. Soc.* **1981**, *103*, 4808. (b) Hermolin, J.; Kosower, E. M. *J. Am. Chem. Soc.* **1981**, *103*, 4813. (c) Fukuzumi, S.; Inada, O.; Satoh, N.; Suenobu, T.; Imahori, H. *J. Am. Chem. Soc.* **2002**, *124*, 9181.

(39) Hirakawa, H.; Kamiya, N.; Kawarabayashi, Y.; Nagamune, T. *Biochim. Biophys. Acta* **2005**, *1748*, 94.